

Waveguide-coupled single NV in diamond enabled by femtosecond laser writing

J. P. HADDEN,^{*,†,‡} V. BHARADWAJ,^{†,¶} B. SOTILLO,[§] S. RAMPINI,[§] R.
 OSELLAME,[§] J. WITMER,^{‡,||} H. JAYAKUMAR,^{‡,⊥} T. T. FERNANDEZ,^{¶,§} A.
 CHIAPPINI,[#] C. ARMELLINI,[#] M. FERRARI,[#] R. RAMPONI,^{¶,§} P. E.
 BARCLAY,[‡] and S. M. EATON^{¶,§}

†These authors contributed equally to this publication

‡Institute for Quantum Science and Technology, University of Calgary, Calgary

¶Department of Physics, Politecnico di Milano, Piazza Leonardo da Vinci 32, Milano, Italy

§Istituto di Fotonica e Nanotecnologie-Consiglio Nazionale delle Ricerche (IFN-CNR),

Piazza Leonardo da Vinci 32, Milano, Italy

||Ginzton Laboratory, Stanford University, Stanford, CA 94305, USA

⊥Department of Physics, City University of New York (CUNY)-City College of New York,

New York, NY 10031, USA

#Istituto di Fotonica e Nanotecnologie (IFN)-CNR, CSMFO and FBK-CMM, Trento, Italy

E-mail: jpe.hadden@gmail.com

Abstract

Diamond's nitrogen vacancy (NV) center is an optically active defect with long spin coherence times, showing potential for efficient nanoscale magnetometry and entanglement schemes. Recently, both the formation of buried 3D optical waveguides and high quality single NVs in diamond were demonstrated using femtosecond laser-writing.

However, until now, combining these technologies has been an outstanding challenge. In this work, we fabricate laser-written photonic circuits in diamond aligned within micron resolution to single laser-written NVs, enabling an integrated platform providing deterministically positioned waveguide-coupled NVs. This fabrication technology opens the way towards on-chip optical routing of single photons between NVs and optically integrated spin-based magnetometry.

Keywords

Waveguides, Laser materials processing, Femtosecond phenomena, Diamond machining, Quantum information and processing, Quantum optics

Diamond's negatively charged nitrogen-vacancy (NV) color center is a point defect consisting of a nearest-neighbor substitutional nitrogen atom and a lattice vacancy. These optically active defects have long room temperature spin coherence times, making them promising for nanoscale magnetic field sensing¹ and for quantum information processing systems.² An integrated photonics platform in diamond would be beneficial for quantum computing based on optically entangled NVs interacting via optical waveguides, as well as NV-based optically detected spin magnetometry, due to the integration and stability provided by monolithic optical waveguides.³

Recently, the versatile femtosecond laser microfabrication method was used to demonstrate buried 3D optical waveguides in diamond,^{4,5} a key step towards a diamond photonics platform. However, for practical implementation of quantum information systems and high spatial resolution magnetometry devices, deterministic placement of NVs is required. The most widely used method to place NV centers in diamond relies on ion implantation followed by annealing.^{6,7} This method offers submicron spatial accuracy and significant progress has been made in the development of annealing processes to repair unwanted damage to the lattice which can degrade the NV centers properties, especially for shallow centers.^{8,9} However the increased energy required for deeper NV creation causes even more damage,¹⁰ thus

techniques which place NV centers in buried structures with minimal damage are preferable.

In 2013, it was shown that NV centers could be produced in optical grade diamond by exploiting the electron plasma created by femtosecond laser pulses focused just above the diamond surface.¹¹ This technique however was limited to near-surface placement of NVs and caused ablative damage of the diamond surface. Recently, Chen *et al.* demonstrated a significant improvement, with on-demand and high quality single NVs written in the bulk of quantum grade diamond (nitrogen concentration of <5 ppb) using femtosecond laser writing with a spatial light modulator (SLM) to correct for aberrations followed by high temperature annealing.^{12,13}

In this Letter, we apply femtosecond laser writing to inscribe optical waveguides and to create single NVs within quantum grade diamond. Crucially, we find that the optical waveguide remains even after the high temperature sample annealing required to form single NVs. Since the same laser and positioning system are used to form both the waveguide mode and NVs, they may be aligned to within micron resolution. We further demonstrate waveguide excitation and collection of light from laser-formed single NVs. Such waveguide coupled NVs could open the door to more sophisticated quantum photonic networks in diamond, exploiting optically linked single NVs for single photon sources or solid state qubits.¹⁴⁻¹⁶ In lower purity diamond, the laser writing of high density NV ensembles within waveguides could enable robust excitation and collection of the fluorescence signal for magnetometry.^{17,18}

The femtosecond laser used for waveguide writing was a regeneratively amplified Yb:KGW system (Pharos, Light Conversion) with 230 fs pulse duration, 515 nm wavelength and 500 kHz repetition. The femtosecond laser pulses were focused below the diamond surface with a 1.25 NA oil immersion lens (RMS100X-O 100× Plan Achromat Oil Immersion Objective, Olympus). Computer-controlled 3-axis motion stages (ABL1000, Aerotech) were used to translate the quantum grade diamond sample (2 mm × 2 mm × 0.3 mm, nitrogen impurities <5 ppb, MB optics) transversely relative to the laser to form the optical waveguides. Figure 1 shows an overhead schematic (a) and optical microscope image (b) of the waveguide-NV

optical device. In order to calibrate the depth and pulse energy of NV formation relative to the waveguide formation depth, multiple test waveguides with NV centers in them were written. In this paper, we focus on one waveguide with NV centers created at the corresponding depth.

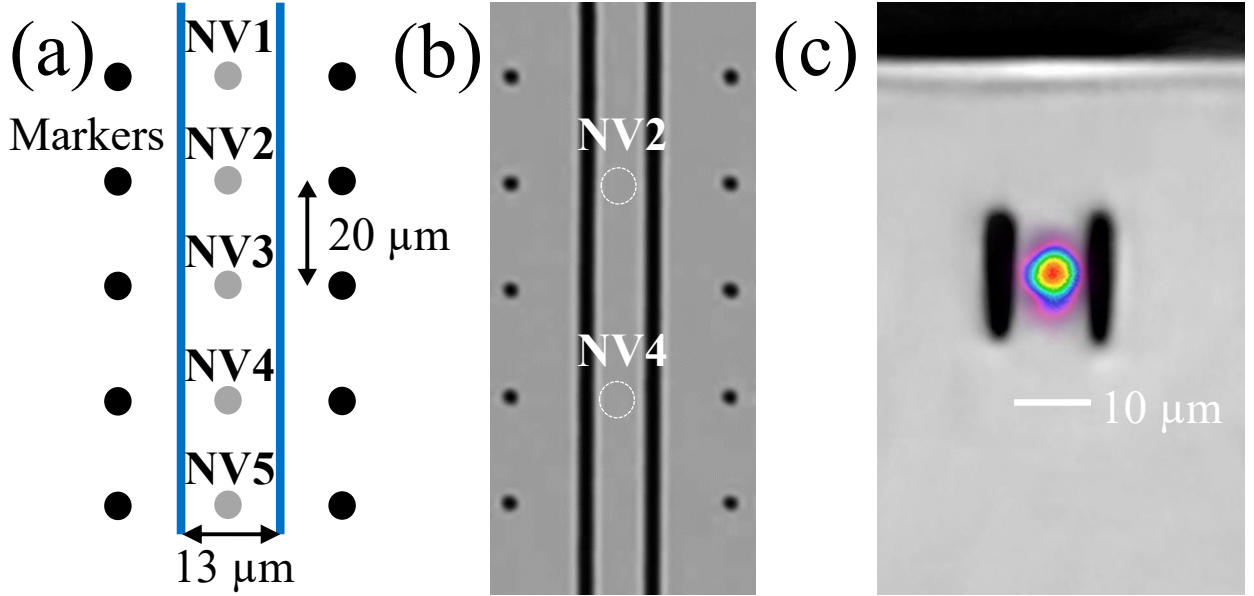


Figure 1: Device overview and waveguide output mode. (a) Overhead schematic of waveguide-NV device, showing five single-pulse femtosecond laser exposures between laser-induced modification lines, with markers outside the waveguide to indicate the position of the single pulse exposures. (b) Overhead optical microscope image of the same area. (c) Transverse optical microscope image of type II waveguide and overlaid 635 nm mode profile.

The optical waveguide was formed at 25 μm depth with processing conditions of 500 kHz repetition rate, 60 nJ pulse energy, and 0.5 mm/s scan speed, corresponding to approximately 1000 pulses within the scanned focal spot. Because focused femtosecond laser pulses yield an amorphization/graphitization in crystalline diamond, the type II geometry¹⁹ was adopted, where two closely spaced laser-written modification lines provide optical confinement. To achieve single mode guiding of visible light, 13 μm separation between the laser-formed modification lines was used. A lower pulse energy was required than in our previous study⁴ because of the shallower depth, resulting in reduced spherical aberration and therefore less distortion in the intensity distribution at the focus.

The near-field intensity profile of the single transverse waveguide mode was measured

by imaging the output facet with a 0.65 NA 60 \times asphere to a CCD (SP620U, Spiricon). The mode field diameter (MFD) for the nearly circular mode was 10 μm at 635 nm wavelength (Fig. 1(c)). MFD measurements were made using the $D4\sigma$ (second moment width) calculation from the beam profiling software (BeamGage, Spiricon), approximately equal to the $1/e^2$ diameter for the nearly Gaussian mode. The insertion loss was 5 dB at 635 nm wavelength (TLS001-635, Thorlabs) for the TM polarization launched with a PM fiber.

Using the same femtosecond laser setup, single-pulse exposures were inscribed within the optical waveguide to induce vacancies in the diamond lattice. The pulse energy used was 28 nJ, below the single pulse damage threshold (~ 50 nJ) in diamond. Five identical static exposures separated by 20 μm were written in order to study reproducibility in forming single NV centers within the waveguiding region. The depth of the static exposures was 25 μm , centered within the cross section of the laser-written waveguide. Markers visible in our imaging system were inscribed (100 nJ pulse energy, 25 pulses) outside of the waveguide to locate the single pulse exposures, which are not visible to wide-field illuminated optical microscopy.

The diamond sample was subsequently annealed in order to form NV centers. Vacancies, which become mobile above 600 $^\circ\text{C}$, are captured by substitutional nitrogen.⁷ In a sample of this type there can be 100-1000 nitrogen impurities present within the $\sim(1 \mu\text{m})^3$ focal volume of the focused femtosecond laser beam. It has been shown that annealing at higher temperatures (1000 $^\circ\text{C}$ and above) can improve the optical linewidths and spin coherence times of the NV centers, as other vacancy complexes which can be detrimental are annealed out.^{8,9} The annealing was performed in a tubular horizontal furnace (LTF15/50/450, Lenton) at 1000 $^\circ\text{C}$ for three hours in a nitrogen atmosphere, to avoid oxidation of the diamond surface.

At such temperatures, the bulk material does not suffer structural changes or graphitization.²⁰ Previous studies in other crystals have shown that high temperature annealing can erase waveguides produced by femtosecond laser irradiation,^{21,22} due to the recovery of the crystalline structure. In the case of diamond, the laser modification lines remain af-

ter annealing, as the lattice is not restored.²³ From μ Raman measurements performed on the laser-induced modification lines, we observed the formation of a higher concentration of graphite nanoclusters after annealing, consistent with other studies.^{23,24}

Even with the increased graphite inside the modification lines, μ Raman shows similar diamond Raman peak width (i.e. crystal quality) and shift (i.e. stress distribution) after annealing. This indicates that the stress within the guiding region is not relieved.²⁵ Crucially for the NV-waveguide device targeted in this work, we found that the mode profile and insertion loss of the annealed waveguides were unaltered, suggesting the temperature required to cause waveguide degradation is higher than that required to form the NVs. Indeed, subsequent low temperature (6K) measurements of the NV centers formed inside the waveguide shows a 0.7 nm splitting of the ZPL indicating that the stress is still present (see supporting information).

Initial overhead photoluminescence (PL) characterization of the laser-written NV centers and their interaction with the waveguide was performed using a homebuilt confocal microscope as shown in Fig. 2(a). A fiber coupled 532 nm laser (CL532-500-L, Crysta-Laser) was focused onto the sample through a 0.8 NA objective (100 \times CFI60 TU Plan Epi ELWD, Nikon) mounted on a closed loop piezo stage (Tritor 101, PiezosystemJena). The induced PL was collected through the same objective, filtered from the excitation and Raman scattered light using a dichroic beam splitter (ZT 532 RDC, Chroma) and long-pass filters (555 nm long-pass, ET 555 LP Chroma, 650 nm long-pass, FELH 0650 Thorlabs) to allow only the NV phonon sideband (PSB) to pass. This light was focused into a single mode fiber, providing the confocal aperture. Detection of the filtered light was performed using avalanche photodiodes (SPQR-14, Perkin-Elmer). Fluorescence could also be directed to a spectrometer (Acton SP-2750, Princeton Instruments), or to an a back-illuminated EMCCD (DU-897U-CS0-#BV iXon Ultra, Andor) through the use of flip mirror 1. An overhead PL confocal scan of the NV2 trial region (positioned as shown in Fig. 2(b)) shows a bright spot corresponding to an NV center between the two bright laser modified lines. Two of the five

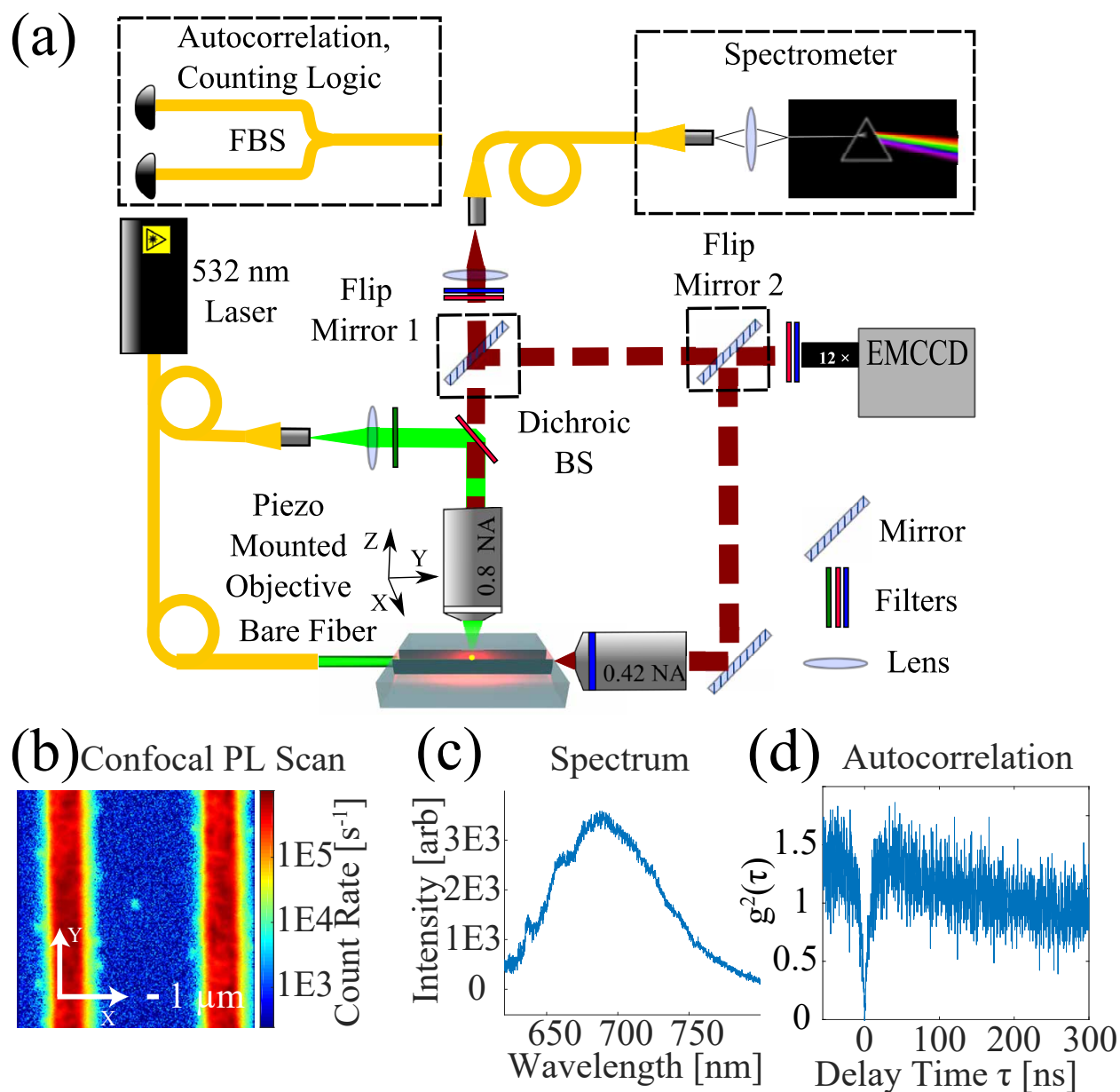


Figure 2: Overhead confocal characterization. (a) Schematic of experimental setup. (b) PL intensity map showing NV2 within the optical waveguide. (c) PL spectrum showing the NV ZPL at 637nm and PSB at longer wavelengths. (d) Intensity autocorrelation revealing single photon emission.

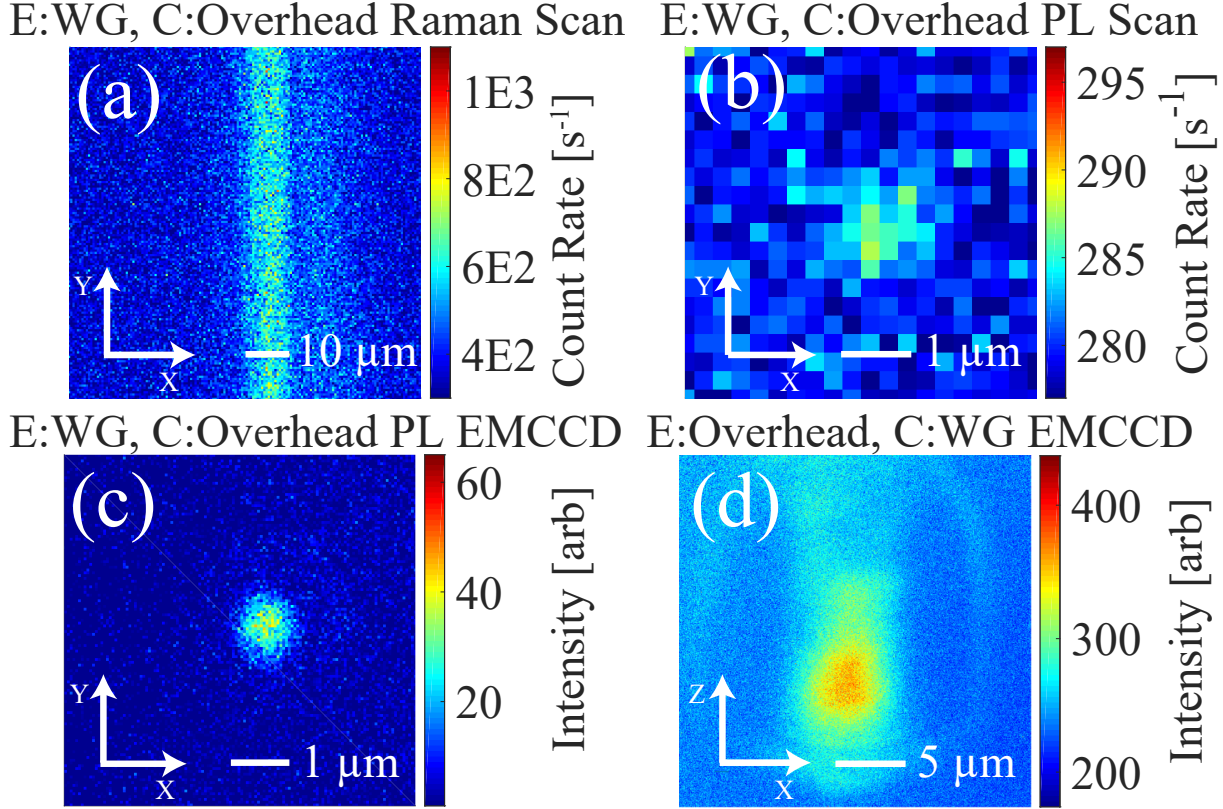


Figure 3: Waveguide excitation and collection of Raman and NV fluorescence. (Titles E: Excitation mode, C: Collection mode) (a) Waveguide excited overhead scan of Raman scattered light. (b) Waveguide excited overhead PL scan of NV2. (c) Waveguide excited overhead PL EMCCD image of NV2. (d) Overhead excited EMCCD intensity image of the of the guided NV emission at the output facet of the optical waveguide.

static exposures in this study (NV2 and NV4) displayed such bright spots after annealing. The single NV formation probability at 28 nJ pulse energy including additional trials in other waveguides was $31 \pm 9 \%$ which is consistent with previous work.¹²

The alignment of the NV centers close to the center of the optical waveguide is important in order for them to be well coupled. We estimate that both NV2 and NV4 are $\sim 1 \mu\text{m}$ shallower than the center of laser-modified lines based on the confocal signal and hence the the optical mode. We selected NV2 for waveguide coupling experiments as its lateral position (shifted by $0.7 \pm 0.3 \mu\text{m}$ from the center of the waveguide, shown in Fig. 2(b)) is better centered compared to NV4 (shifted by $0.9 \pm 0.3 \mu\text{m}$). The $\sim 1 \mu\text{m}$ shift of the NV2 and NV4 is larger than the maximum shifts of $\sim 600 \text{ nm}$ reported previously,¹² which we attribute to

the larger focal volume provided by our femtosecond beam delivery setup. All measurements reported below refer to NV2. Despite being written with three orders of magnitude greater fluence as compared to static exposures, NV centers were also formed in the vicinity of the laser modification lines making up the optical waveguide (Fig. 2(b)). This effect is due to the lower intensity in the wings of the focused Gaussian laser, and was also observed using picosecond laser irradiation of diamond.²⁶

Figure 2(c) shows the PL spectrum recorded from the NV with the 650 nm long-pass filter removed, where the characteristic ZPL at 637 nm and the broadband PSB are clearly visible. An intensity autocorrelation measurement $g^{(2)}(\tau)$ of this is shown in Fig. 2(d), with $g^{(2)}(0)$ well below 0.5, characteristic of single photon emission.

In order to demonstrate the ability to guide 532 nm excitation light through the waveguide to the NV center, the output from the excitation laser was coupled to the laser-written waveguide by butt-coupling a bare single mode fiber (460HP, Thorlabs) to the input facet of the diamond waveguide as shown in Fig. 2(a). Index matching oil was used to improve the transmission and coupling stability. A fraction of the light within the waveguide undergoes Raman scattering, with the first order Raman scattered light shifted to 572 nm. Some of this scattered light is emitted out of the waveguide, and can be detected through the confocal microscope’s collection arm with the 650 nm long-pass filter removed in order to image the guiding properties of the waveguide. Figure 3(a) shows an overhead collection scan of the waveguide, revealing the Raman scattering due to the waveguided excitation light. The waveguide alignment was optimized by monitoring the output intensity at the output facet of the waveguide using a 0.42 NA objective (50× Plan Apo SL Infinity Corrected, Mitutoyo) coupled to a CCD.

Waveguide coupled excitation of the NV center is demonstrated in Fig. 3(b) and (c), with collection of the NV center’s emitted light through the overhead confocal microscope. An overhead confocal collection scan of a small area around NV2 with waveguide excitation shows fluorescence from the expected NV position (Fig. 3(b)). Verification is achieved by

imaging the NV fluorescence with an EMCCD, which again shows emission located at the NV position (Fig. 3(c)). The relatively modest detected photon count rate of 10 counts/s, above the background in Fig. 3(b) is expected given that the mode size of the waveguide ($\sim 5.8 \mu\text{m}$ FWHM) is much larger than the focused spot from free space excitation 0.8 NA lens, ($\sim 0.8 \mu\text{m}$) resulting in a ~ 0.02 reduction in power density at the NV center, in addition to coupling or waveguide losses before it reaches the NV center. Comparable count rates to the confocal microscope collection rate would be expected for similar power densities. An increase in the effective power density could be achieved by tailoring the refractive index profile of the written waveguide to achieve a smaller MFD, or more powerful excitation.

Further evidence of waveguide-NV coupling is shown in Fig. 3(d) where the NV center is excited from above through the confocal microscope's objective, while emission is collected through the optical waveguide. The waveguide output facet is imaged onto the EMCCD through a 0.42 NA objective and using flip mirror 2 (as shown in Fig. 2 (a)). The signal was filtered using a 650 nm long-pass filter, and corrected for any remaining background by subtracting the recorded signal when exciting the waveguide near the NV center. The intensity distribution of the NV emission at the waveguide output (Fig. 3(d)) shows a similar size and shape as the output mode when coupling a 635 nm wavelength laser diode to the waveguide (Fig. 1(c)). An estimate of the coupling efficiency to the waveguide mode relative to the total emission yields 9×10^{-4} , which is a factor of ~ 0.03 less than for our confocal microscope objective (See supporting information). An increase in this coupling efficiency would occur for smaller MFD waveguides.

In summary, we have demonstrated an integrated quantum photonic chip in diamond, fabricated entirely with femtosecond laser writing. The optical waveguides and static exposures to produce vacancies were fabricated in a single processing step, to within micron alignment. We verified through confocal microscopy that single NVs could be formed in quantum grade diamond at depths shallower than $30 \mu\text{m}$ without a SLM compensating for spherical aberration.¹²

Importantly, we showed that optical waveguides could be used to excite and collect light from single NVs. Further improvement in NV excitation and waveguide coupling efficiency is to be expected through reducing the mode size through optimization of the geometry of the type II waveguide. Optical waveguides coupled to NV centers with arbitrary 3D configurations and integrated in quantum grade diamond could open the door for exciting new possibilities in quantum information processing. Future work will study the formation of NV ensembles in lower grade diamond¹⁸ which will boost the waveguided fluorescence signal, as well as the incorporation of bragg grating waveguides²⁷ for more efficient sensing of magnetic fields.

Acknowledgement

The authors acknowledge support from FP7 DiamondFab CONCERT Japan project, DIAMANTE MIUR-SIR grant, FemtoDiamante Cariplo ERC reinforcement grant, University of Calgary's Eyes High Postdoctoral Fellowship program, NSERC Discovery Grant, NSERC Discovery Accelerator Supplement, NSERC Research Tools and Instruments, CFI. We thank Prof. Guglielmo Lanzani and Dr. Luigino Criante for the use of the FemtoFab facility at CNST - IIT Milano for the laser fabrication experiments.

References

- (1) Taylor, J. M.; Cappellaro, P.; Childress, L.; Jiang, L.; Budker, D.; Hemmer, P. R.; Yacoby, A.; Walsworth, R.; Lukin, M. D. High-sensitivity diamond magnetometer with nanoscale resolution. *Nature Phys.* **2008**, *4*, 810–816.
- (2) Hensen, B. et al. Loophole-free Bell inequality violation using electron spins separated by 1.3 kilometres. *Nature* **2015**, *526*, 682–686.
- (3) Schröder, T.; Mouradian, S. L.; Zheng, J.; Trusheim, M. E.; Walsh, M.; Chen, E. H.;

- Li, L.; Bayn, I.; Englund, D. Quantum nanophotonics in diamond. *J. Opt. Soc. Am. B* **2016**, *33*, B65.
- (4) Sotillo, B. et al. Diamond photonics platform enabled by femtosecond laser writing. *Sci. Rep.* **2016**, *6*, 35566.
- (5) Courvoisier, A.; Booth, M. J.; Salter, P. S. Inscription of 3D waveguides in diamond using an ultrafast laser. *Appl. Phys. Lett.* **2016**, *109*, 031109.
- (6) Orwa, J. O.; Santori, C.; Fu, K. M. C.; Gibson, B.; Simpson, D.; Aharonovich, I.; Stacey, A.; Cimmino, A.; Balog, P.; Markham, M.; Twitchen, D.; Greentree, A. D.; Beausoleil, R. G.; Prawer, S. Engineering of nitrogen-vacancy color centers in high purity diamond by ion implantation and annealing. *J. Appl. Phys.* **2011**, *109*, 083530.
- (7) Rabeau, J. R.; Reichart, P.; Tamanyan, G.; Jamieson, D. N.; Prawer, S.; Jelezko, F.; Gaebel, T.; Popa, I.; Domhan, M.; Wrachtrup, J. Implantation of labelled single nitrogen vacancy centers in diamond using N15. *Appl. Phys. Lett.* **2006**, *88*, 023113.
- (8) Naydenov, B.; Reinhard, F.; Lämmle, A.; Richter, V.; Kalish, R.; D’Haenens-Johansson, U. F. S.; Newton, M.; Jelezko, F.; Wrachtrup, J. Increasing the coherence time of single electron spins in diamond by high temperature annealing. *Appl. Phys. Lett.* **2010**, *97*, 242511.
- (9) Yamamoto, T. et al. Extending spin coherence times of diamond qubits by high-temperature annealing. *Phys. Rev. B* **2013**, *88*, 075206.
- (10) Pezzagna, S.; Naydenov, B.; Jelezko, F.; Wrachtrup, J.; Meijer, J. Creation efficiency of nitrogen-vacancy centres in diamond. *New J. Phys.* **2010**, *12*, 065017.
- (11) Liu, Y.; Chen, G.; Song, M.; Ci, X.; Wu, B.; Wu, E.; Zeng, H. Fabrication of nitrogen vacancy color centers by femtosecond pulse laser illumination. *Opt. Express* **2013**, *21*, 12843.

- (12) Chen, Y.-C.; Salter, P. S.; Knauer, S.; Weng, L.; Frangeskou, A. C.; Stephen, C. J.; Ishmael, S. N.; Dolan, P. R.; Johnson, S.; Green, B. L.; Morley, G. W.; Newton, M. E.; Rarity, J. G.; Booth, M. J.; Smith, J. M. Laser writing of coherent colour centres in diamond. *Nat. Photon.* **2016**, *11*, 77–80.
- (13) Sotillo, B.; Bharadwaj, V.; Hadden, J.; Rampini, S.; Chiappini, A.; Fernandez, T.; Armellini, C.; Serpengüzel, A.; Ferrari, M.; Barclay, P.; Ramponi, R.; Eaton, S. Visible to Infrared Diamond Photonics Enabled by Focused Femtosecond Laser Pulses. *Micromachines* **2017**, *8*, 60.
- (14) Kimble, H. J. The Quantum Internet. *Nature* **2008**, *453*, 1023–1030.
- (15) Shi, Q.; Sontheimer, B.; Nikolay, N.; Schell, A. W.; Fischer, J.; Naber, A.; Benson, O.; Wegener, M. Wiring up pre-characterized single-photon emitters by laser lithography. *Sci. Rep.* **2016**, *6*, 31135.
- (16) Sipahigil, A. et al. An integrated diamond nanophotonics platform for quantum-optical networks. *Science* **2016**, *354*, 847–850.
- (17) Gazzano, O.; Becher, C. Highly Sensitive On-Chip Magnetometer with Saturable Absorbers in Two-Color Microcavities. *arXiv preprint arXiv:1603.04529* **2016**,
- (18) Clevenson, H.; Trusheim, M. E.; Teale, C.; Schröder, T.; Braje, D.; Englund, D. Broad-band magnetometry and temperature sensing with a light-trapping diamond waveguide. *Nature Phys.* **2015**, *11*, 393–397.
- (19) Burghoff, J.; Grebing, C.; Nolte, S.; Tünnermann, A. Efficient frequency doubling in femtosecond laser-written waveguides in lithium niobate. *Appl. Phys. Lett.* **2006**, *89*, 081108.
- (20) Meng, Y.-F.; Yan, C.-S.; Lai, J.; Krasnicki, S.; Shu, H.; Yu, T.; Liang, Q.; Mao, H.-I.; Hemley, R. J. Enhanced optical properties of chemical vapor deposited single crystal

- diamond by low-pressure/high-temperature annealing. *Proc. Natl. Acad. Sci. U.S.A.* **2008**, *105*, 17620–17625.
- (21) Benayas, A.; Jaque, D.; McMillen, B.; Chen, K. P. Thermal stability of microstructural and optical modifications induced in sapphire by ultrafast laser filamentation. *J. Appl. Phys.* **2010**, *107*, 033522.
- (22) Ródenas, A.; Torchia, G. A.; Lifante, G.; Cantelar, E.; Lamela, J.; Jaque, F.; Roso, L.; Jaque, D. Refractive index change mechanisms in femtosecond laser written ceramic Nd:YAG waveguides: micro-spectroscopy experiments and beam propagation calculations. *Appl. Phys. B* **2009**, *95*, 85–96.
- (23) Kalish, R.; Reznik, A.; Praver, S.; Saada, D.; Adler, J. Ion-Implantation-Induced Defects in Diamond and Their Annealing: Experiment and Simulation. *Phys. Status Solidi A* **1999**, *174*, 83–99.
- (24) Ferrari, A. C.; Robertson, J. Interpretation of Raman spectra of disordered and amorphous carbon. *Phys. Rev. B* **2000**, *61*, 14095–14107.
- (25) Olivero, P.; Bosia, F.; Fairchild, B. A.; Gibson, B. C.; Greentree, A. D.; Spizzirri, P.; Praver, S. Splitting of photoluminescent emission from nitrogen vacancy centers in diamond induced by ion-damage-induced stress. *New J. Physics* **2013**, *15*, 043027.
- (26) Pimenov, S. M.; Khomich, A. A.; Neuenschwander, B.; Jäggi, B.; Romano, V. Picosecond-laser bulk modification induced enhancement of nitrogen-vacancy luminescence in diamond. *JOSA b* **2016**, *33*, B49–B55.
- (27) Bharadwaj, V.; Courvoisier, A.; Fernandez, T. T.; Ramponi, R.; Galzerano, G.; Nunn, J.; Booth, M. J.; Osellame, R.; Eaton, S. M.; Salter, P. S. Femtosecond laser inscription of Bragg grating waveguides in bulk diamond. *Arxiv Prepr. arXiv:1705.10285* **2017**,

Graphical TOC Entry

